International Core Journal of Engineering Volume 7 Issue 5, 2021
ISSN: 2414-1895 DOI: 10.6919/ICJE.202105_7(5).0048

Analytical Model of E-core Coil Impedance Eddy Current

Chenghao Xu

School of Shanghai Maritime University, Shanghai 201306, China.

1546837842@qq.com

Abstract

This template explains and demonstrates how to prepare your camera-ready paper for Tran. In this paper, the TREE method is used to establish the impedance calculation model of the E-core coil above the conductor plate with cylindrical through hole. This method divides the entire area into different partition interfaces, and uses the relationship between the partition interfaces to finally obtain the closed form expression of the E-core coil impedance. Introduced the Dichotomy-Newton method to solve non-complex zeros. In MATLAB, the E-core coil impedance is calculated under the excitation of alternating current with a frequency from 0.1KHz to 100KHz. The results show that with the increase of frequency, the existence of cylindrical through the hole makes the comparison between the real part of impedance and the non-porous conductor plate show small first, then large, and finally tend to be equal. At the same time, the analytical calculation results in MATLAB are consistent with the simulation calculation results using Maxwell finite element very good, verified the correctness of the algorithm.

Keywords

Eddy Current Testing; E-core; Truncated Region Equation Expansion Method (TREE); Impedance Calculation; Finite Element Simulation.

1. Introduction

The difference in the position of the magnetic core causes the impedance of the eddy current probe to change, and the magnetic core in the center has a better magnetization ability and improves the sensitivity of the coil to detect defects in the conductor plate [1-5]. For different magnetic core shapes, some scholars have proposed the truncated region characteristic equation expansion method (TREE), which can calculate important parameters such as the impedance of the magnetic core coil, the current density of the conductor plate, and the vector magnetic potential [6-9]. At the same time, this method can also be applied to the situation that there are defects on the surface of the conductor plate [10-12]. When applying the TREE method, it is very important to obtain the zero point in the specific function expression. The accuracy of the zero point directly affects the calculation result, Newton-Raphson The Newton-Raphson Method can be applied to find the complex zero point [13,14]. This paper establishes an impedance analytical calculation model for the coil with air-gap E core located on the through-hole conductor plate, and analyzes the influence of the through hole of the conductor plate and the magnetic core on the impedance component of the coil. The change of the impedance component is used to judge the defect of the conductor plate quantitatively. An important basis for evaluation. This paper also introduces the bisection-Newton method to solve non-complex zeros. Other documents have not conducted a separate analysis on the calculation of the E core coil for the cylindrical through-hole conductor plate and the non-complex zero point.

ISSN: 2414-1895 DOI: 10.6919/ICJE.202105_7(5).0048

2. Theoretical Analysis

Figure 1 depicts the air-gap E magnetic core coil located above the cylindrical through-hole conductor plate. Truncated region equation expansion method is applied. This method cuts the entire model into different areas. The Dirichlet boundary condition is used when the radius reaches a certain value. , Suppose the magnetic vector intensity in the radial direction is zero. The physical meaning is that when the radius reaches a certain value, the magnetic vector intensity A_φ is very small, which can be regarded as 0 under ideal conditions.

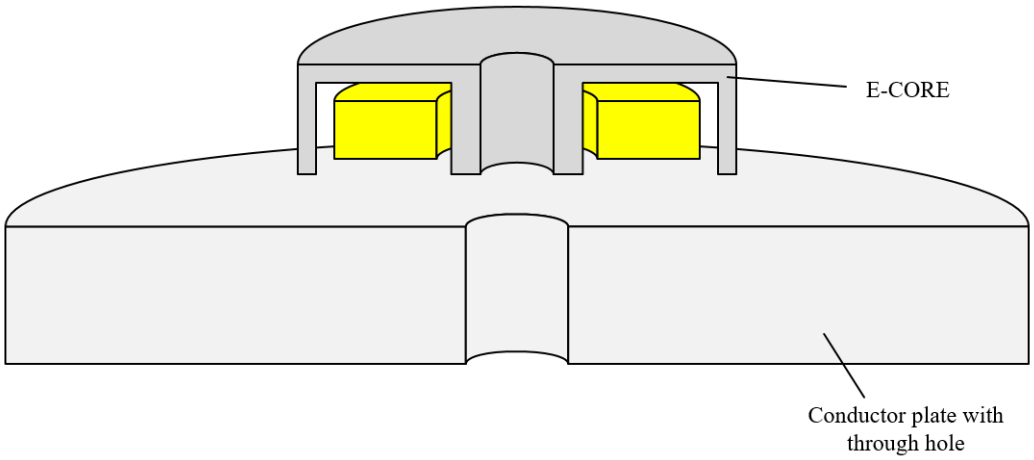

Figure 1. The E core coil with air hole is located above the conductor plate with through hole

Figure 2 describes the axisymmetric model of the E-core coil. The excitation is a sinusoidal current $Ie^{j\omega t}$ applied to a single-turn coil. The coil is wound on the E core of relative permeability μ_f. The entire coil is located on a conductor plate with a cylindrical through hole. The size of the through hole is g, and the relative permeability μ_r and electrical conductivity of the conductor plate is σ_r, respectively. The *TREE* method cuts off the entire model into different regions, using Dirichlet boundary conditions when the radius reaches a certain value, set the magnetic vector strength in the radius direction to 0. The physical meaning is that when the radius reaches a certain value, the magnetic vector strength is very small, which can be regarded as 0 under ideal conditions. The entire axisymmetric model is divided into 6 layers. The problem of this model can be regarded as a typical boundary value and continuous electromagnetic field problem. Through the separation of variables method, the magnetic vector potential of different regions can be expressed by general mathematical expressions:

$$A(r,z) = \sum_{i=1}^{\infty} [A_i J_1(q_i r) + B_i Y_1(q_i r)][C_i e^{-s_i z} + D_i e^{s_i z}] \quad (1)$$

Where J_i and Y_i are the Bessel function of i order and $s_i = (q_i^2 + j\omega\mu_0\mu_r\sigma_i)^{1/2}$. The unknown coefficents A_i, B_i, C_i, D_i, and the discrete eigenvalues q_i are to be determined from the boundary and interface conditions. When in areas 1 and 5, because of Y_i the divergence at the origin, the displacement magnetic potential A is bounded, B_i=0.When r=b, the vector magnetic potential $A_\varphi(b,z)$=0, so the discrete eigenvalues q_i can be calculated:

$$J_1(q_i b) = 0 \quad (2)$$

When in region 2, the air layer can be divided into three sub-regions I, II, and III. The vector magnetic potential A of these three sub-regions can be expressed as follows:

$$\begin{aligned} A_I(r) &= A_E J_1(m_i r) && 0 \le r \le a_1 \\ A_{\mathrm{II}}(r) &= A_E B_{2F} J_1(m_i r) + A_E C_{2F} Y_1(m_i r) && a_1 \le r \le c_2 \\ A_{\mathrm{III}}(r) &= A_E B'_{2F} J_1(m_i r) + A_E C'_{2F} Y_1(m_i r) && c_2 \le r \le b \end{aligned} \quad (3)$$

ISSN: 2414-1895 DOI: 10.6919/ICJE.202105_7(5).0048

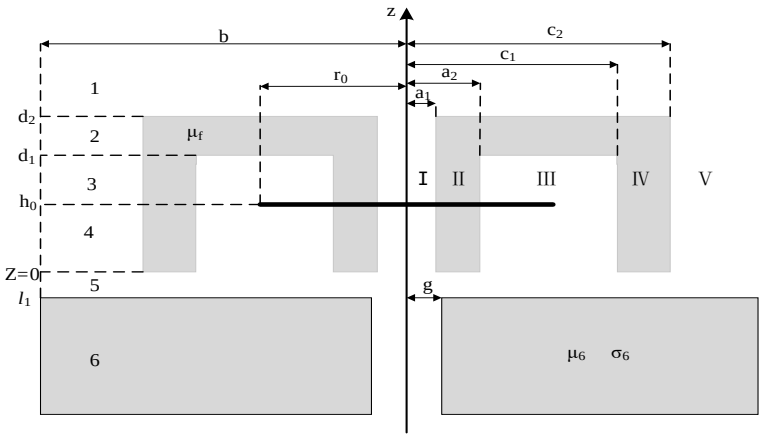

Figure 2. E core single-turn coil model

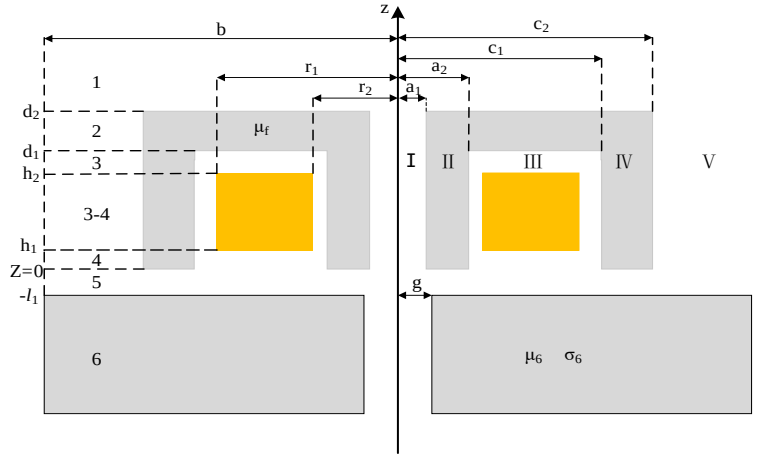

Figure 3. E core multi-turn coil model

By determining the boundary conditions of r=a_1 and r=c_2, the boundary conditions are the continuity of B_z and H_r or A_φ and $\partial A_\varphi/\partial z$, and the values of the unknowns coefficents B_{2F}, C_{2F}, B'_{2F}, C'_{2F} in (3) are determined by the orthogonality of the Bessel function. At the same time $A_\varphi(b,z)$ =0, the value of m_i can be determined.

$$L'_1(m_i b) = 0 \tag{4}$$

Where

$$L'_n(m_i r) = B'_{2F} J_n(m_i r) + C'_{2F} Y_n(m_i r) \tag{5}$$

Continuity through boundary conditions B_z and H_r.

$$B'_{2F} = -\frac{\pi}{2} m_i c_2 \left[\frac{Y_1 L_0(m_i c_2)}{\mu_f} - Y_0(m_i c_2) L_1(m_i c_2)\right] \tag{6}$$

$$C'_{2F} = \frac{\pi}{2} m_i c_2 \left[\frac{J_1(m_i c_2) L_0(m_i c_2)}{\mu_f} - J_0(m_i c_2) L_1(m_i c_2)\right] \tag{7}$$

$$L_n(m_i r) = B_{2F} J_n(m_i r) + C_{2F} Y_n(m_i r) \tag{8}$$

$$B_{2F} = \frac{\pi}{2} m_i a_1 \left[J_1(m_i a_1) Y_0(m_i a_1) - \mu_f J_0(m_i a_1) Y_1(m_i a_1)\right] \tag{9}$$

$$C_{2F} = \frac{\pi}{2} m_i a_1 \left[(\mu_f - 1) J_0(m_i a_1) J_1(m_i a_1)\right] \tag{10}$$

In regions 3 and 4, there are a total of 5 sub-areas, the sub-areas are I~V. At the same time, through $A_\varphi(b,z)$ =0, the value of can be determined. The vector magnetic potential of the sub-region along the radius can be expressed as

ISSN: 2414-1895 DOI: 10.6919/ICJE.202105_7(5).0048

$$\begin{array}{cc} A_I(r) = A_E J_1(p_i r) & 0 \le r \le a_1 \\ A_{II}(r) = A_E B_{3F} J_1(p_i r) + A_E C_{3F} Y_1(p_i r) & a_1 \le r \le a_2 \\ A_{III}(r) = A_E B'_{3F} J_1(p_i r) + A_E C'_{3F} Y_1(p_i r) & a_2 \le r \le c_1 \\ A_{IV}(r) = A_E B''_{3F} J_1(p_i r) + A_E C''_{3F} Y_1(p_i r) & c_1 \le r \le c_2 \\ A_V(r) = A_E B'''_{3F} J_1(p_i r) + A_E C'''_{3F} Y_1(p_i r) & c_2 \le r \le b \end{array} \quad (11)$$

The value of the discrete eigenvalue can be obtained by calculating the equation of (1.12)

$$R_1'''(p_i b) = 0 \quad (12)$$

In the same way, the unknowns B_{3F}, C_{3F}, B'_{3F}, C'_{3F}, B'_{3F}, C'_{3F}, B'''_{3F}, and C'''_{3F} can be calculated through the continuity of the boundary conditions B_z and H_r.

$$R_n'''(p_i r) = B'''_{3F} J_n(p_i r) + C'''_{3F} Y_n(p_i r) \quad (13)$$

$$B'''_{3F} = -\frac{\pi}{2} p_i c_2 \left[\frac{Y_1(p_i c_2) R_0''(p_i c_2)}{\mu_f} - Y_0(p_i c_2) R_1''(p_i c_2) \right] \quad (14)$$

$$C'''_{3F} = \frac{\pi}{2} p_i c_2 \left[\frac{J_1(p_i c_2) R_0''(p_i c_2)}{\mu_f} - J_0(p_i c_2) R_1''(p_i c_2) \right] \quad (15)$$

$$R_n''(p_i r) = B''_{3F} J_n(p_i r) + C''_{3F} Y_n(p_i r) \quad (16)$$

$$B''_{3F} = \frac{\pi}{2} p_i c_1 \left[R'_1(p_i c_1) Y_0(p_i c_1) - \mu_f R'_0(p_i c_1) Y_1(p_i c_1) \right] \quad (17)$$

$$C''_{3F} = \frac{\pi}{2} p_i c_1 \left[\mu_f R'_0(p_i c_1) J_1(p_i c_1) - R'_1(p_i c_1) J_0(p_i c_1) \right] \quad (18)$$

$$R_n'(p_i r) = B'_{3F} J_n(p_i r) + C'_{3F} Y_n(p_i r) \quad (19)$$

$$B'_{3F} = -\frac{\pi}{2} p_i a_2 \left[\frac{Y_1(p_i a_2) R_0(p_i a_2)}{\mu_f} - Y_0(p_i a_2) R_1(p_i a_2) \right] \quad (20)$$

$$C'_{3F} = \frac{\pi}{2} p_i a_2 \left[\frac{J_1(p_i a_2) R_0(p_i a_2)}{\mu_f} - J_0(p_i a_2) R_1(p_i a_2) \right] \quad (21)$$

$$R_n(p_i r) = B_{3F} J_n(p_i r) + C_{3F} Y_n(p_i r) \quad (22)$$

$$B_{3F} = \frac{\pi}{2} p_i a_1 [J_1(p_i a_1) Y_0(p_i a_1) - \mu_f J_0(p_i a_1) Y_1(p_i a_1)] \quad (23)$$

$$C_{3F} = \frac{\pi}{2} p_i a_1 \left[(\mu_f - 1) J_0(p_i a_1) J_1(p_i a_1) \right] \quad (24)$$

In region 6, the magnetic potential of the conductor plate with through-holes in the radial direction can be expressed as:

$$A(r) = A_u [Y_1(v_i b) J_n(v_i r) - J_1(v_i b) Y_n(v_i r)] \quad (25)$$

$$P_n(v_i r) = Y_1(v_i b) J_n(v_i r) - J_1(v_i b) Y_n(v_i r) \quad (26)$$

Through (25) and (26), the expressions of the magnetic potential $\boldsymbol{A}_{hole}(r)$ and $\boldsymbol{A}_{plate}(r)$ along the radius of the conductor plate with or without through holes can be obtained:

$$\boldsymbol{A}_{\text{hole}}(r) = A_u J_1(u_i r) P_1(v_i g) \quad (27)$$

$$A_{\text{plate}}(r) = A_u P_1(v_i r) J_1(u_i g) \quad (28)$$

Where g is the radius of the through hole and u_i is the discrete characteristic value of area 6, $v_i = \sqrt{u_i^2 - j\omega\mu_r\mu_0\sigma}$. When r=g, it can be determined by boundary conditions:

$$u_i P_1(v_i g) J_1(u_i g) = \frac{1}{\mu_r} v_i J_1(u_i g) P_1(v_i g) \quad (29)$$

By calculating (29), the value of the discrete eigenvalue u_i can be obtained, which also satisfies $A_{plate}(b) = 0$ when r=b. Finally, the vector magnetic potential expressions in all different layers are transformed into a matrix form:

$$\boldsymbol{A}_1(r,z) = J_1(\boldsymbol{q}^T r) \boldsymbol{q}^{-1} e^{-\boldsymbol{q}z} \boldsymbol{C_1} \quad (30)$$

$$\boldsymbol{A}_2(r,z) = \begin{array}{cc} J_1(\boldsymbol{m}^T r) & 0 \le r \le a_1 \\ L_1(\boldsymbol{m}^T r) \boldsymbol{m}^{-1} (e^{-\boldsymbol{m}z} \boldsymbol{C}_2 - e^{\boldsymbol{m}z} \boldsymbol{B}_2) & a_1 \le r \le c_2 \\ L'_1(\boldsymbol{m}^T r) & c_2 \le r \le b \end{array} \quad (31)$$

ISSN: 2414-1895 DOI: 10.6919/ICJE.202105_7(5).0048

$$\boldsymbol{A}_3(r,z)=R_1'(\boldsymbol{p}^Tr)\boldsymbol{p}^{-1}(e^{-pz}\boldsymbol{C}_3-e^{pz}\boldsymbol{B}_3)\begin{cases}J_1(\boldsymbol{p}^Tr) & 0\le r\le a_1\\ R_1(\boldsymbol{p}^Tr) & a_1\le r\le a_2\\ R_1'(\boldsymbol{p}^Tr) & a_2\le r\le c_1\\ R_1''(\boldsymbol{p}^Tr) & c_1\le r\le c_2\\ R_1'''(\boldsymbol{p}^Tr) & c_2\le r\le b\end{cases} \tag{32}$$

$$\boldsymbol{A}_4(r,z)=R_1'(\boldsymbol{p}^Tr)\boldsymbol{p}^{-1}(e^{-pz}\boldsymbol{C}_4-e^{pz}\boldsymbol{B}_4)\begin{cases}J_1(\boldsymbol{p}^Tr) & 0\le r\le a_1\\ R_1(\boldsymbol{p}^Tr) & a_1\le r\le a_2\\ R_1'(\boldsymbol{p}^Tr) & a_2\le r\le c_1\\ R_1''(\boldsymbol{p}^Tr) & c_1\le r\le c_2\\ R_1'''(\boldsymbol{p}^Tr) & c_2\le r\le b\end{cases} \tag{33}$$

$$\boldsymbol{A}_5(r,z)=J_1(\boldsymbol{q}^Tr)\boldsymbol{q}^{-1}(e^{-\boldsymbol{pz}}\boldsymbol{C}_5-e^{\boldsymbol{pz}}\boldsymbol{B}_5) \tag{34}$$

$$\boldsymbol{A}_6(r,z)=-\begin{matrix}J_1(\boldsymbol{u}^Tr)P_1(\boldsymbol{v}g) & 0\le r\le g\\ P_1(\boldsymbol{v}^Tr)J_1(\boldsymbol{u}g) & g\le r\le b\end{matrix}\boldsymbol{u}^{-1}e^{\boldsymbol{uz}}\boldsymbol{B}_6 \tag{35}$$

Where $J_1(\boldsymbol{q}^Tr)$, $J_1(\boldsymbol{m}^Tr)$, $L_1(\boldsymbol{m}^Tr)$, $L_1'(\boldsymbol{m}^Tr)$, $J_1(\boldsymbol{p}^Tr)$, $R_1(\boldsymbol{p}^Tr)$, $R_1'(\boldsymbol{p}^Tr)$, $R_1''(\boldsymbol{p}^Tr)$, $J_1(\boldsymbol{u}^Tr)$, $R_1'''(\boldsymbol{p}^Tr)$, $P_1(\boldsymbol{v}g)$, $P_1(\boldsymbol{v}^Tr)$, $J_1(\boldsymbol{u}g)$ are row vectors. $\boldsymbol{q},\boldsymbol{m},\boldsymbol{p},\boldsymbol{u},\boldsymbol{v},e^{\pm\boldsymbol{pz}},e^{\pm\boldsymbol{mz}},e^{\boldsymbol{uz}}$ are diagonal matrixes, unknown coefficients $\boldsymbol{C}_i$ and $\boldsymbol{B}_i$are column vector. The unknown coefficient $\boldsymbol{C}_i$ and $\boldsymbol{B}_i$ is determined by the boundary relationship between adjacent layers. The boundary condition is the continuity of B_z and H_r. Using the orthogonality of the Bessel function, the simplification can calculate the mutual relationship between $\boldsymbol{C}_i$ and $\boldsymbol{B}_i$, and then calculate the vector magnetic potential $\boldsymbol{A}_\varphi(r,z)$, where the mutual relationship is as follows:

$$\begin{matrix}\boldsymbol{C}_{56}\\ \boldsymbol{B}_{56}\end{matrix}=\frac{1}{2}e^{\mp\boldsymbol{q}l_1}\boldsymbol{E}^{-1}(\boldsymbol{W}\mp\boldsymbol{K})e^{-\boldsymbol{u}l_1} \tag{36}$$

$$\begin{matrix}\boldsymbol{C}_{\boldsymbol{46}}\\ \boldsymbol{B}_{\boldsymbol{46}}\end{matrix}=\frac{1}{2}\boldsymbol{D}^{-1}\left[\left(\boldsymbol{G}'\pm\boldsymbol{H}'\right)\boldsymbol{C}_{\boldsymbol{56}}+\left(\boldsymbol{G}'\mp\boldsymbol{H}'\right)\boldsymbol{B}_{\boldsymbol{56}}\right] \tag{37}$$

$$\begin{matrix}\boldsymbol{C}_{26}\\ \boldsymbol{B}_{26}\end{matrix}=\frac{1}{2}\boldsymbol{F}^{-1}e^{\pm\boldsymbol{m}d_1}[(\boldsymbol{G}\pm\boldsymbol{H})e^{-\boldsymbol{p}d_1}\boldsymbol{C}_{\boldsymbol{46}}+(\boldsymbol{G}\mp\boldsymbol{H})e^{\boldsymbol{p}d_1}\boldsymbol{B}_{\boldsymbol{46}}] \tag{38}$$

$$\boldsymbol{\lambda}_1=\frac{1}{2}\boldsymbol{A}\boldsymbol{F}^{-1}e^{\boldsymbol{m}d_1}\left[(\boldsymbol{G}+\boldsymbol{H})e^{-\boldsymbol{p}d_1}e^{\boldsymbol{p}h_0}+(\boldsymbol{G}-\boldsymbol{H})e^{\boldsymbol{p}d_1}e^{-\boldsymbol{p}h_0}\right] \tag{39}$$

$$\boldsymbol{\lambda}_2=\frac{1}{2}\boldsymbol{A}\boldsymbol{F}^{-1}e^{-\boldsymbol{m}d_1}\left[(\boldsymbol{G}-\boldsymbol{H})e^{-\boldsymbol{p}d_1}e^{\boldsymbol{p}h_0}+(\boldsymbol{G}+\boldsymbol{H})e^{\boldsymbol{p}d_1}e^{-\boldsymbol{p}h_0}\right] \tag{40}$$

Where the matrices $\boldsymbol{D}$, $\boldsymbol{F}$, $\boldsymbol{E}$ are diagonal matrices, and $\boldsymbol{W}$, $\boldsymbol{K}$, $\boldsymbol{G}$, $\boldsymbol{H}$, $\boldsymbol{G}'$, $\boldsymbol{H}'$ are full matrices.

$$\boldsymbol{A}=\frac{1}{2}\mu_0 I\boldsymbol{D}^{-1}r_0R_1'(\boldsymbol{p}r_0) \tag{41}$$

$$\boldsymbol{C}_{i6}=\frac{\boldsymbol{C}_i}{\boldsymbol{B}_6} \tag{42}$$

$$\boldsymbol{B}_{i6}=\frac{\boldsymbol{B}_i}{\boldsymbol{B}_6} \tag{43}$$

In order to calculate the expression $\boldsymbol{A}_\varphi$of the coil in Figure 3, the superposition principle can be applied to obtain its expression. The coil is composed of a finite width $(r_2-r_1)$and a finite height (h_2-h_1). The vector magnetic potential $\boldsymbol{A}(r,z)$ can be integrated along the rectangular cross-section of the cylindrical coil through the magnetic vector potential $\boldsymbol{A}_{filamentary}(r,z)$ of the single-turn coil to obtain the expressions of the N-turn vector magnetic potentials of different partitions. Let the expression $\boldsymbol{A}_3(r,z)$ in Figure 3 be $h_2=z$ and $\boldsymbol{A}_4(r,z)$ be $h_1=z$, add the two formulas to obtain the vector magnetic potential expression $\boldsymbol{A}_{3,4}(r,z)$, and calculate the corresponding resistance by dividing the N-turn coil along the rectangular cross-sectional area of the cylindrical coil. The formula is:

$$Z=\frac{j\omega\oint\boldsymbol{A}_{3,4}(r,z)\cdot dl}{I}=\frac{j\omega 2\pi r\boldsymbol{A}_{3,4}(r,z)}{I} \tag{44}$$

Through the calculation of formula (44), the impedance of the N-turn coil can be obtained, and the coil expression is:

ISSN: 2414-1895 DOI: 10.6919/ICJE.202105_7(5).0048

$$Z = \frac{j w p\ m_0 N^2}{(r_2 - r_1)^2 (h_2 - h_1)^2} \mathrm{Int}(\mathbf{p}^T r_1, \mathbf{p}^T r_2) \mathbf{p}^{-4} \cdot \{2(h_2 - h_1)\mathbf{p} + e^{\mathbf{p}(h_1 - h_2)} - e^{\mathbf{p}(h_2 - h_1)} + \left[\left(e^{-\mathbf{p}h_1} - e^{-\mathbf{p}h_2}\right)\mathbf{C_{46}} - \left(e^{-\mathbf{p}h_1} - e^{-\mathbf{p}h_2}\right)\mathbf{B_{46}} \right] \cdot \mathbf{M} \} \mathbf{p}^{-3} \mathbf{D}^{-1} \mathrm{Int}(\mathbf{p}r_1, \mathbf{p}r_2) \quad (45)$$

In formula (45):

$$\boldsymbol{Int}(\boldsymbol{p}r_1, \boldsymbol{p}r_2) = \int_{\boldsymbol{p}r_1}^{\boldsymbol{p}r_2} r\, R_0'(\boldsymbol{p}r) dr \quad (46)$$

$$i_0 = \frac{NI}{(r_2 - r_1)(h_2 - h_1)} \quad (47)$$

$$\boldsymbol{M} = [(\boldsymbol{T} - \boldsymbol{U})e^{-\boldsymbol{m}d_2}\boldsymbol{C_{27}} - (\boldsymbol{T} + \boldsymbol{U})e^{\boldsymbol{m}d_2}\boldsymbol{B_{27}}]^{-1} \times [(\boldsymbol{T} + \boldsymbol{U})e^{\boldsymbol{m}d_2}\boldsymbol{\lambda_2} - (\boldsymbol{T} - \boldsymbol{U})e^{-\boldsymbol{m}d_2}\boldsymbol{\lambda_1}] \quad (48)$$

3. Results and Analysis

In the TREE method, it is very important to obtain the discrete feature roots in equations (2), (4), (12) and (29). The accuracy of the feature roots directly affects the calculation results. In order to find an effective method to automatically search for characteristic roots, different forms of characteristic roots can be divided into two categories. The first type is the real roots of the characteristic functions related to the core radius and permeability obtained through boundary conditions at the magnetic core position. The characteristic roots of equations (2), (4) and (12) are all real numbers. The use of the bisection-Newton algorithm can speed up the convergence speed and obtain the zero point in the specified interval. When using Newton's method to calculate, the zero point after iteration may exceed the specified interval or the iteration speed will be slow. When using Newton's method does not work, use the dichotomy method, readjust the zero point interval and then judge until the error of the zero point value obtained by Newton's method or dichotomy method is less than the required accuracy, then the zero point of the interval is obtained.

The characteristic roots of the second type in the characteristic function obtained through the boundary conditions for the through-hole conductor plate are in the form of complex roots, and the characteristic roots of equation (29) are all complex numbers. The basic method for calculating complex roots is Newton-Raphson Method.

The parameters of the coil, magnetic core and conductor plate are shown in Table 1. The solution domain radius b=54 mm is 12 times the outer radius of the coil, and the sum term is 76 items (N_s=76). The determination of b and N_s were found in [6].

Table 1. Parameters of coils, magnetic cores and conductor plates

Coil		Ferrite core		Plate	
Inner coil r_1	3.0mm	Inner column a_1	1.2mm	Conductivity σ	10.0 MS m^{-1}
Outer coil r_2	4.5mm	Outer column a_2	2.6mm	Domain b	54mm
Offset l_1	0.01mm	Inner core c_1	5mm	Hole g	2.5mm
Length $h_2 - h_1$	2.025mm	Outer core c_2	6mm		
Numbers of turns N	500	Inner core height d_1	2.6mm		
		Outer core height d_2	4mm		

Discrete eigenvalues u_i can be determined by the Newton-Raphson method in the literature [13,14]. The integral in equation (46) is realized by using the Struve(), besselj(), bessely() functions, and expanding the Struve function and the Bessel function.

Calculate the formula (45) to get the impedance value $Z = R + jX$ of the through-hole conductor plate. The air core coil assumes μ_f=0, the calculated impedance value. In the case of a non-conductor plate, set the conductivity σ =0, and let $\boldsymbol{u} = \boldsymbol{q}$, $\boldsymbol{W} = \boldsymbol{E}$ and $\boldsymbol{K} = -\boldsymbol{E}$ can obtain the impedance value $Z_0 = R_0 + jX_0$ of the non-conductor plate. The change of the real part of the impedance is $\Delta R_0 = R - R_0$, and the change of the imaginary part of the impedance is $\Delta X_0 = X - X_0$.

ISSN: 2414-1895 DOI: 10.6919/ICJE.202105_7(5).0048

Keep the through-hole conductor plate unchanged, change the relative permeability of the magnetic core μ_f=0, you can get the impedance of the air core coil, and calculate the impedance change value. When the frequency changes from 0.1kHz to 100kHz, the real part of the impedance change in Figure 4 first increases with the frequency. After reaching the frequency f_R= 10KHz, the impedance change reaches the maximum and then begins to decrease. It can be seen from Figure 5 that the E magnetic core has little effect on the change trend of impedance, but a larger impedance change is obtained. The maximum relative difference between the real part calculated by the impedance TREE method and the simulation does not exceed 1.5%, and the maximum imaginary part does not exceed 0.45%. It can be seen that the TREE method calculation and the impedance normalized change value obtained by the simulation method are in good agreement. The inductance calculated by impedance analysis is L=0.701H when there is an E-shaped magnetic core (f =1KHz), and the inductance calculated by analysis is L_0=0.18H without a magnetic core.

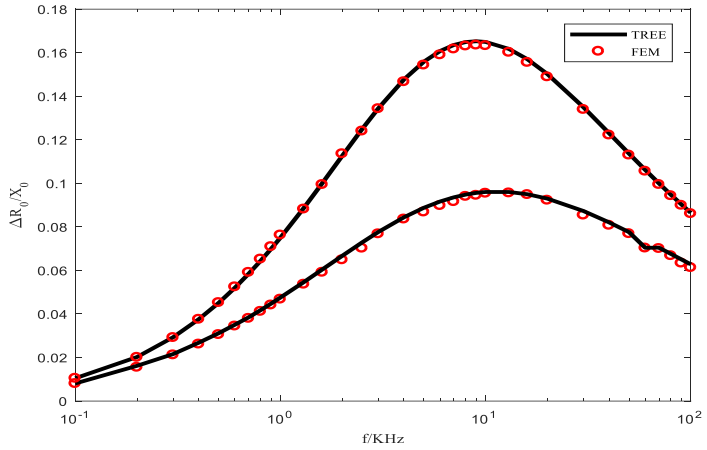

Figure 4. Comparison of the relationship between the normalized resistance value of the air core and the E core coil and the frequency

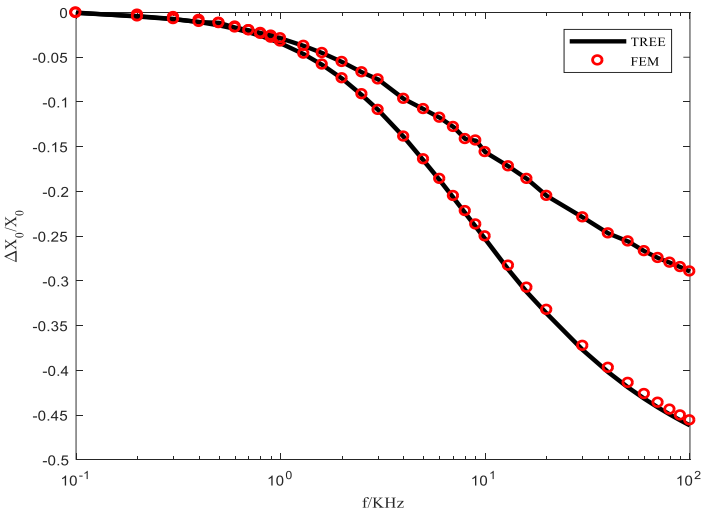

Figure 5. Comparison of the relationship between the normalized reactance value and frequency of air core and E core coil

Equations (49) and (50) can calculate the relative difference of coil impedance between E core and air core. The results of some frequencies are shown in Table 2. With or without a magnetic core, the maximum change of the real part of the impedance is δ_R=84.368%, and the maximum change of the imaginary part is δ_X=72.974%. The magnetization of the E magnetic core makes the impedance change large.

ISSN: 2414-1895 DOI: 10.6919/ICJE.202105_7(5).0048

$$\delta_R = \frac{R_{\text{without core}} - R_{\text{core}}}{R_{\text{without core}}} \cdot 100\% \tag{49}$$

$$\delta_X = \frac{X_{\text{without core}} - X_{\text{core}}}{X_{\text{without core}}} \cdot 100\% \tag{50}$$

Table 2. The existence of E magnetic core has an effect on the relative difference between coil impedance

f/khz	δ_R [%]	δ_X [%]
0.1	82.647	72.974
1	83.157	72.832
10	84.368	69.477
50	81.728	65.412
100	80.846	64.384

Keeping the magnetic core unchanged, by comparing the impedance relationship between the complete conductor plate and the conductor plate with cylindrical through-holes, the influence of the cylindrical through-hole on impedance changes can be obtained. To calculate the complete conductor plate, you need to change the expression $\boldsymbol{C}_{56}$ and $\boldsymbol{B}_{56}$:

$$\begin{matrix}\boldsymbol{C}_{56}\\ \boldsymbol{B}_{56}\end{matrix} = \frac{1}{2} e^{\mp \boldsymbol{q} l_1} (\boldsymbol{I} \mp \boldsymbol{q} s_6^{-1}) e^{-s_6 l_1} \tag{51}$$

Incorporating equation (51) into equation (37) can obtain the impedance expression of the through-hole conductor plate. Figures 6 and 7 respectively show the normalized values of the real and imaginary parts of the impedance of the coil with respect to the reactance of the complete conductor plate coil with respect to the cylindrical through hole of the conductor plate. The maximum relative error between the two results obtained from analytical calculation and finite element simulation does not exceed 1.6%. From an intuitive analysis, when the frequency is small, the presence of through holes in the conductor plate reduces the eddy current density on the surface, resulting in a change in the impedance of the conductor plate with through holes in the real part of less than zero. As the frequency increases, the skin effect increases, so that the eddy current is concentrated on the surface, resulting in the change of the real part of the impedance of the through-hole conductor plate being greater than 0, and finally the eddy current is concentrated on the surface and the impedance change tends to be equal.

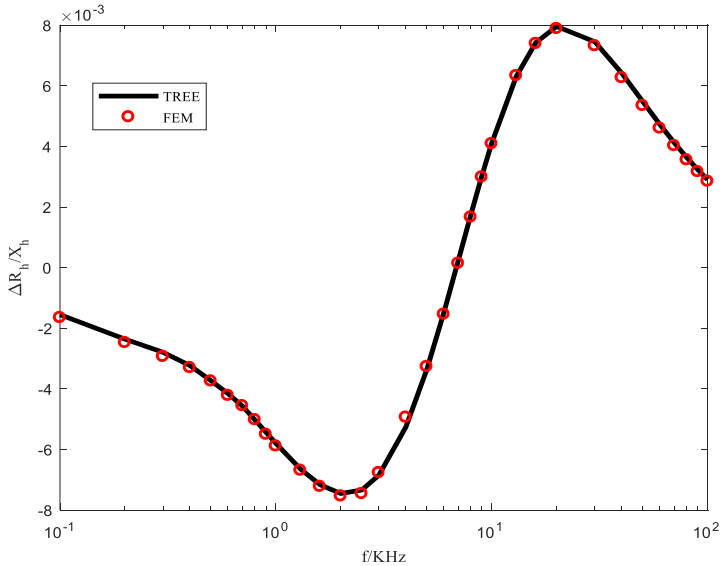

Figure 6. The relationship between the normalized resistance value of the through-hole conductor plate coil and the frequency

ISSN: 2414-1895 DOI: 10.6919/ICJE.202105_7(5).0048

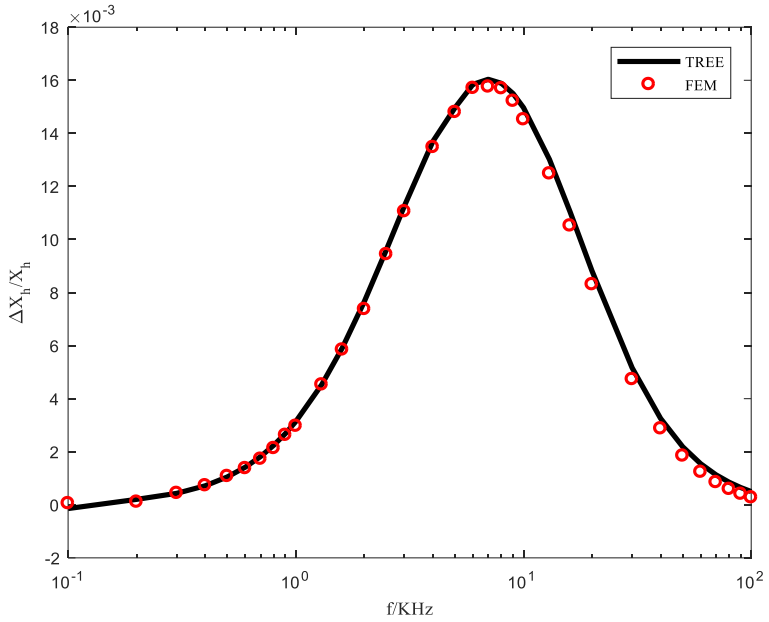

Figure 7. The relationship between the normalized reactance value of the through-hole conductor plate coil and the frequency

4. Conclusion

In this paper, the characteristic function expansion method of the truncated area is used to calculate the impedance of the E core coil above the conductor plate with the through hole radius g. The final closed form expression can be calculated in MATLAB, and the calculated error can be controlled by changing the value of the solution domain radius b or changing the number of the summation term Ns. By comparing with the result of finite element simulation, the result of impedance change is verified. When the coil is close to the conductive material, the change of the coil impedance component of the E magnetic core is much larger than that without the magnetic core. The existence of the magnetic core increases the density of the magnetic flux in the conductive material and ensures the high efficiency of detecting defects.

References

[1] Wang Xiaolei, Ji Zhigang, Guo Xiangqian et al. Current situation and development trend of non-destructive testing technology for maintenance and remanufacturing of coal mine machinery equipment[J] Science Technology and Engineering, 2021, 21(2):423-433.

[2] Xu Jin. A frequency selection method for parameter measurement of the metallic multi-layer plate using eddy current[J]. Science Technology and Engineering, 2020, 20(5):1895-1899.

[3] Zhang Siquan. Analytical Analysis of the Influence of Ferrite Core Position on Impedance Change of Eddy Current Probe[J]. Chinese Journal of Sensors and Actuators, 2020(6):791-795.

[4] Zhang Siquan, Tang jiangfeng. Theory Verification of Changing the Distribution of Eddy Current Inside Conductor by a New Phase Shifted Fields Probe. Chinese Journal of Sensors and Actuators, 2016, 29(8): 1169-1175.

[5] Zhang Siquan, Hu Shengbin, Lu Wenhua. The Series Expansions Calculation Model for the Impedance of Coil above Arbitrary Layer Conductive Plates[J]. Chinese Journal of Sensors and Actuators, 2011 (11): 1596-1601.

[6] T.P. Theodoulidis, A model of ferrite-cored probes 3078.

[7] Tytko, G. and Dziczkowski, L. An analytical model of an I-cored coil with a circular air gap, IEEE Transactions on Magnetics,2017, Vol. 53 No. 4.

ISSN: 2414-1895 DOI: 10.6919/ICJE.202105_7(5).0048

[8] H. Bayani, T. P. Theodoulidis, and I. Sasada, Application of Eigenfunction Expansions to Eddy Current (NDE): A Model of Cup-Cored Probes, IOP Press, London, UK, 2007, pp. 57–64.

[9] F. Sakkaki and H. Bayani, Solution to the problem of E-cored coil above a layered half-space using the method of truncated region eigenfunction expansion, J. Appl. Phys., vol. 2012,111, no. 7, p. 07E717,

[10] T. P. Theodoulidis and E. E. Kriezis, Eddy Current Canonical Problems (With Applications to Nondestructive Evaluation). Forsyth, GA, USA: Tech Science Press, 2006, pp. 93–135.

[11] Tytko, G., Dziczkowski, L. An analytical model of an I-cored coil located above a conductive material with a hole. European Physical Journal Applied Physics, 2018, 82 (2), 21001.

[12] G. Tytko and L. Dziczkowski, E-cored coil with a circular air gap inside the core column used in eddy current testing, IEEE Trans. Mag., Sep. 2015, vol. 51, no. 9, Art. no. 6201804.

[13] Abramowitz M. Stegun I. A. Handbook of Mathematical Functions (with formulas, graphs and mathematical tables), Dover, 1970, New York.

[14] T. P. Theodoulidis, J.R. Bowler. Eddy-Current interaction of a long coil with a slot in a conductive plate[J]. IEEE Trans.Magn, 2005, VOL.41(9):1238-1247.